Actin binding to WH2 domains regulates nuclear import of the multifunctional actin regulator JMY

J. Bradley Zuchero, Brittany Belin, and R. Dyche Mullins
Cellular and Molecular Pharmacology, University of California, San Francisco, San Francisco, CA 94158; Physiology Course, Marine Biological Laboratory, Woods Hole, MA 02543

ABSTRACT **Junction-mediating and regulatory protein (JMY) is a regulator of both transcription and actin filament assembly. In response to DNA damage, JMY accumulates in the nucleus and promotes p53-dependent apoptosis. JMY's actin-regulatory activity relies on a cluster of three actin-binding Wiskott–Aldrich syndrome protein homology 2 (WH2) domains that nucleate filaments directly and also promote nucleation activity of the Arp2/3 complex. In addition to these activities, we find that the WH2 cluster overlaps an atypical, bipartite nuclear localization sequence (NLS) and controls JMY's subcellular localization. Actin monomers bound to the WH2 domains block binding of importins to the NLS and prevent nuclear import of JMY. Mutations that impair actin binding, or cellular perturbations that induce actin filament assembly and decrease the concentration of monomeric actin in the cytoplasm, cause JMY to accumulate in the nucleus. DNA damage induces both cytoplasmic actin polymerization and nuclear import of JMY, and we find that damage-induced nuclear localization of JMY requires both the WH2/NLS region and importin β. On the basis of our results, we propose that actin assembly regulates nuclear import of JMY in response to DNA damage.**

Monitoring Editor
Thomas D. Pollard
Yale University

Received: Dec 3, 2011
Revised: Jan 6, 2012
Accepted: Jan 9, 2012

INTRODUCTION

Junction-mediating and regulatory protein (JMY) leads a double life in vertebrate cells. In the cytoplasm it promotes actin filament assembly and contributes to cell migration (Zuchero *et al.*, 2009), whereas in the nucleus it acts as a transcriptional coactivator and promotes programmed cell death in response to DNA damage (Shikama *et al.*, 1999; Coutts *et al.*, 2007). The connection between these distinct cellular functions has remained mysterious.

JMY's effects on actin assembly require its C-terminal WWWCA region, composed of three, tandem actin monomer–binding sequences (Wiskott–Aldrich syndrome protein homology 2 [WH2] domains) and an Arp2/3-binding central and acidic (CA) region. Similar to WH2-CA domains found in Wiskott–Aldrich syndrome protein–family proteins, this region of JMY can promote actin nucleation by the Arp2/3 complex (Welch and Mullins, 2002). In addition, the cluster of WH2 domains can also nucleate actin filaments by itself, using a mechanism remarkably similar to that of the spire-family proteins (Quinlan *et al.*, 2005). In slow-moving cells (e.g., fibroblasts) endogenous JMY occurs in both the nucleus and the cytoplasm, but in highly motile cells (e.g., neutrophils), it is predominantly cytoplasmic and specifically enriched at the leading edge. Both the rate of cell migration and the cytoplasmic concentration of filamentous actin increase when JMY is overexpressed and decrease when JMY expression is knocked down by RNA interference (RNAi; Zuchero *et al.*, 2009). The JMY-dependent increase in cell motility requires its Arp2/3-binding region and is not observed when JMY localization is restricted to the nucleus (Coutts *et al.*, 2009; Zuchero *et al.*, 2009) either by DNA damage or by fusion to a strong nuclear localization sequence (NLS). In nerve cells, JMY appears to suppress neurite outgrowth, an activity that requires its intrinsic actin nucleation activity (Firat-Karalar *et al.*, 2011). Of interest, actin assembly by the Arp2/3 complex also suppresses neurite outgrowth and axon migration in nerve cells (Strasser *et al.*, 2004). Taken together, the data indicate that JMY regulates cell shape and motility, at least in part, by promoting actin assembly in the cytoplasm.

This article was published online ahead of print in MBoC in Press (http://www.molbiolcell.org/cgi/doi/10.1091/mbc.E11-12-0992) on January 19, 2012.

Address correspondence to: R. Dyche Mullins (dyche@mullinslab.ucsf.edu).

Abbreviations used: ABD, actin-binding domain; Impα, importin α; Impβ, importin β; jasp, jasplakinolide; JMY, junction-mediating and regulatory protein; LatB, latrunculin B; LMB, leptomycin B; NLS, nuclear localization signal; WH2, Wiskott–Aldrich syndrome protein homology 2 domain.

In response to DNA damage, JMY accumulates in the nucleus, where it enhances transcription by the tumor suppressor p53 and promotes apoptosis (Shikama *et al.*, 1999; Coutts *et al.*, 2007). Three additional proteins are known to modulate JMY's nuclear function: the acetyltransferase p300, an adaptor protein called Strap, and the ubiquitin ligase Mdm2. In the nucleus, JMY forms a complex with p300 and Strap that is believed to acetylate p53 and increase its proapoptotic transcriptional activity. Mdm2 can oppose this activity by promoting degradation of both JMY and p53. Given growing evidence that actin has important functions in the nucleus, including regulation of transcription, it is tempting to speculate that JMY might make actin filaments in the nucleus. There is, however, no evidence to support this idea.

To understand the connection between its nuclear and cytoplasmic functions, we investigated the mechanism by which JMY translocates from the cytoplasm into the nucleus. Surprisingly, we find that decreases in the cytoplasmic concentration of monomeric actin drive translocation of JMY into the nucleus and that actin-dependent translocation is controlled by the cluster of WH2 domains. We identified a bipartite nuclear localization sequence that partially overlaps the WH2 cluster and found that WH2 mutations that prevent actin binding are sufficient to drive JMY into the nucleus. In vitro, monomeric actin bound to the WH2 domains blocks access of the importin α/β (Impα/β) complex to JMY's NLS. This mechanism of regulation is remarkably similar to that of the myocardin-related transcription factor (MRTF) proteins, whose nuclear localization is also actin dependent but which use an unrelated actin-binding sequence called a RPEL domain. The lack of sequence similarity and the evolutionary history of JMY argue strongly that the similarities in MRTF and JMY regulation represent a case of convergent evolution. Of interest, DNA damage–induced nuclear accumulation of JMY absolutely requires the actin-sensitive nuclear localization sequence embedded in the WWWCA domain. We find that DNA damage sufficient to produce nuclear accumulation of JMY also induces incorporation of monomeric actin into cytoplasmic filaments incapable of binding JMY. Our work argues strongly that nuclear translocation of JMY in response to DNA damage is an actin-dependent process.

RESULTS

Identification of proteins with both a putative actin-binding domain and NLS

To identify factors that might link actin dynamics to nuclear events, we searched the human genome for coding sequences containing one or more potential actin-binding domains and at least one predicted nuclear localization sequence (Nair *et al.*, 2003). We tested both actin monomer-binding (WH2 and RPEL) and filament-binding (calponin homology, formin homology 2, ILWEQ, and ezrin/radixin/moesin) sequences and identified 28 proteins that met our criteria (Supplemental Table S1). Of interest, in 14 of these proteins the predicted actin-binding domain (ABD) overlaps or is adjacent to the NLS (Figure 1A). This motif occurs in several well-known actin monomer–binding proteins (JMY, MRTF proteins, Phactr1-4, Scar2/WAVE2), formin-family members (Daam1-2, Diaph1, Fhod3), canonical adhesion proteins (ezrin, radixin, moesin, talin), and others, including SYNE/nesprin proteins, dystonin, neuron navigator, and huntingtin interacting protein 1.

We used cell fractionation and fluorescence microscopy to test whether the proteins with overlapping ABD and NLS sequences shuttle between the cytoplasm and nucleus and whether their localization depends on the state of the actin cytoskeleton. We treated cells with jasplakinolide (jasp) to polymerize actin and reduce the cytoplasmic concentration of actin monomers (Bubb *et al.*, 1994, 2000; Kiuchi *et al.*, 2011), latrunculin B (LatB) to depolymerize actin filaments and increase monomer concentration (Spector *et al.*, 1983; Lyubimova *et al.*, 1997), or leptomycin B (LMB) to inhibit exportin1/Crm1–dependent nuclear export (Wolff *et al.*, 1997). We then fractionated cells into cytoplasmic and nuclear pools and assessed protein localization by immunoblotting (Supplemental Figure S1A). Probes against cytoplasmic (HSP70) and nuclear (lamin B1) markers demonstrate the efficiency of fractionation (Figure 1B and Supplemental Figure S1A). When suitable antibodies were not available, we expressed candidates as green fluorescent protein (GFP) fusions (including MAL and Phactr1) and analyzed localization by fluorescence microscopy (Supplemental Figure S1B).

Actin regulates the subcellular localization of JMY

Of the 14 proteins we tested, only three exhibit changes in localization as a function of actin assembly/disassembly: JMY, MAL (also known as MRTF-A and MKL1), and Phactr1. Consistent with previous reports (Vartiainen *et al.*, 2007), MAL accumulates in the nucleus in response to jasp and LMB and in the cytoplasm in response to LatB (Supplemental Figure S1B, top). Phactr1, another RPEL motif–containing protein (Sagara *et al.*, 2009), accumulates in the nucleus in response to jasp (Supplemental Figure S1B, bottom, and c) and colocalizes with actin-based structures in the cytoplasm (Supplemental Figure S1D). It is striking that both endogenous and GFP-tagged JMY also accumulate in the nucleus in response to jasp (fold increase in nuclear JMY, 2.45 ± 0.62 SEM; in GFP-JMY, 2.68 ± 0.14; Figure 1, B and C, and Supplemental Figure S1A). We confirmed these results by fluorescence microscopy of GFP-JMY in live cells (Figure 1, D and E). GFP-JMY was enriched in the nucleus of only 2.2 ± 1.1% of mock-treated cells (78.6 ± 5.4% predominantly cytoplasmic), and treatment with jasp increased this localization by almost 10-fold (19.0 ± 2.4% nuclear; 31.3 ± 2.7% cytoplasmic). In contrast to MAL, however, we observed no change in JMY localization in response to LMB or LatB (Supplemental Figure S1A; see also later discussion of Figure 3).

Does the actin-dependent localization of JMY depend on its ability to bind actin monomers? To test this, we made point mutations in JMY WH2 domains (where [A*B*C*] refers to mutations made in WH2-a, -b, and -c) previously shown to compromise actin binding (Quinlan *et al.*, 2005; Kelly *et al.*, 2006). We validated these mutations in vitro using pyrene actin assembly assays (Supplemental Figure S2, A and B). Consistent with the effects of jasp, compromising the ability of all three WH2 domains to bind actin (GFP-JMY[A*B*C*]) causes JMY to become completely nuclear (Figure 1F). Putative NLS-2 overlaps both the C-terminal LRKT motif of WH2-a and the linker connecting it to WH2-b (Supplemental Figure S2C), and so we tested the effect of mutating only the first two WH2 domains. Similar to the [A*B*C*] triple mutant, the double mutant GFP-JMY[A*B*] also accumulates in the nucleus despite being able to bind actin on WH2-c (Figure 1F and Supplemental Figure S2, A and B). These results suggest that actin monomers bound to WH2-a and -b block JMY nuclear import by masking NLS-2.

To understand the function and regulation of JMY's putative NLS regions, we tested their function by fusing them to GFP. The nuclear pore complex has a mesh size of ~2.6 nm and, in the absence of a functional NLS, GFP (Stokes radius, 2.4 nm) equilibrates slowly between the nucleus and cytoplasm (Mohr *et al.*, 2009). Accordingly, we find GFP distributed equally between cytoplasm and nucleus (predominantly nuclear in 4.9% of cells). Its localization shifts to the nucleus when fused to either a control NLS from the SV40 large T antigen (98.5% nuclear), JMY NLS-1 (95.6% nuclear), or JMY NLS-2 (83.2% nuclear; Figure 1, G and H). This demonstrates that both JMY NLS-1 and -2 are functional.

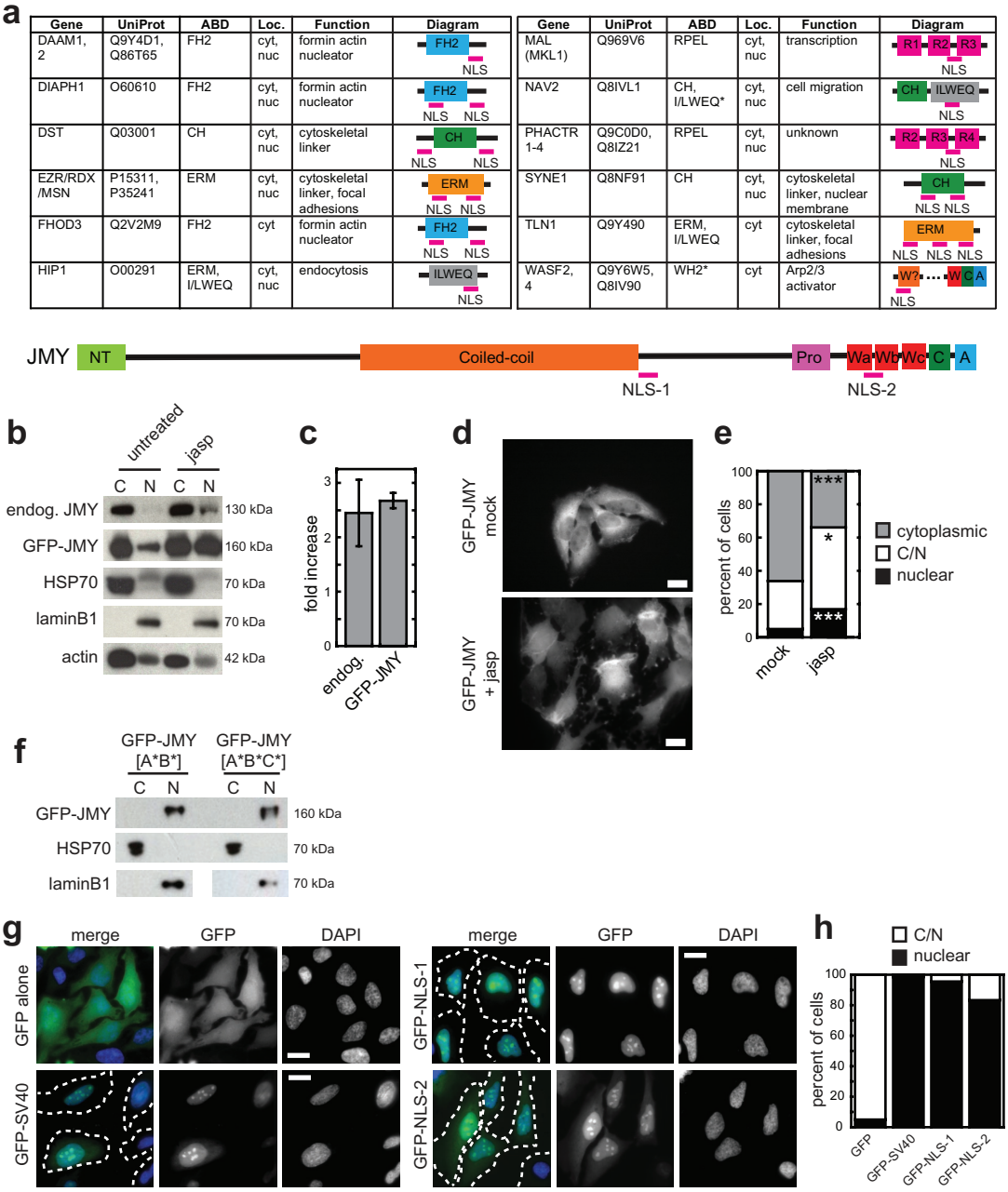

FIGURE 1: Actin regulates the subcellular localization of JMY. (A) Proteins with overlap between putative NLS and ABDs. The table indicates Uniprot number (http://www.uniprot.org), type of ABD, cellular localization (Loc.), function, and a diagram showing position of the putative NLS relative to the ABD. References and full gene names are found in Supplemental Table S1. Asterisk indicates putative (uncharacterized) ABD. Bottom, domain structure of JMY, showing position of putative NLSs (NLS-1, amino acids 603–620; NLS-2, 867–882). WH2s are abbreviated Wa, Wb, and Wc. Other domains illustrated are as follows: NT, N-terminal; Pro, polyproline; C, Central; A, acidic (Zuchero *et al.*, 2009). (B, C) Endogenous and GFP-JMY accumulate in the nucleus following polymerization of actin with 500 nM jasp for 30 min. Following drug treatment, wild-type cells or cells stably expressing GFP-JMY were fractionated into cytoplasmic and nuclear pools (see *Materials and Methods*). Immunoblotting was performed to assess the localization of JMY, and fraction purity was determined by blotting with HSP70 (cytoplasmic marker) and lamin B1 (nuclear marker). (C) Quantification of immunoblots indicates that both endogenous and GFP-tagged JMY are ~2.5 times more nuclear in jasp-treated cells relative to untreated cells. Error bars, SEM; n ≥ 3. (D, E) Analysis of GFP-JMY localization by microscopy. GFP-JMY accumulates in the nucleus in response to actin polymerization induced by jasplakinolide. JMY constructs were transiently expressed in HeLa cells for 16 h prior to treatment with jasp or DMSO (mock). (E) Quantification of ≥300 cells per condition, n ≥ 3, showing percentage of cells that were predominantly cytoplasmic (gray), equally distributed in cytoplasm and nucleus (C/N, white) or predominantly nuclear (black). *p < 0.05, ***p < 0.005. (F) Actin-binding mutants GFP-JMY[A*B*] and GFP-JMY[A*B*C*] are completely nuclear. Cells were transfected and fractionated as in B. n = 2. (G, H) JMY NLS-1 and NLS-2 are functional NLS sequences. Tagging GFP with either a control NLS (SV40) or JMY NLS drives it into the nucleus. (G) Quantification of GFP localization in ≥130 cells per condition, n = 2. All scale bars, 20 μm.

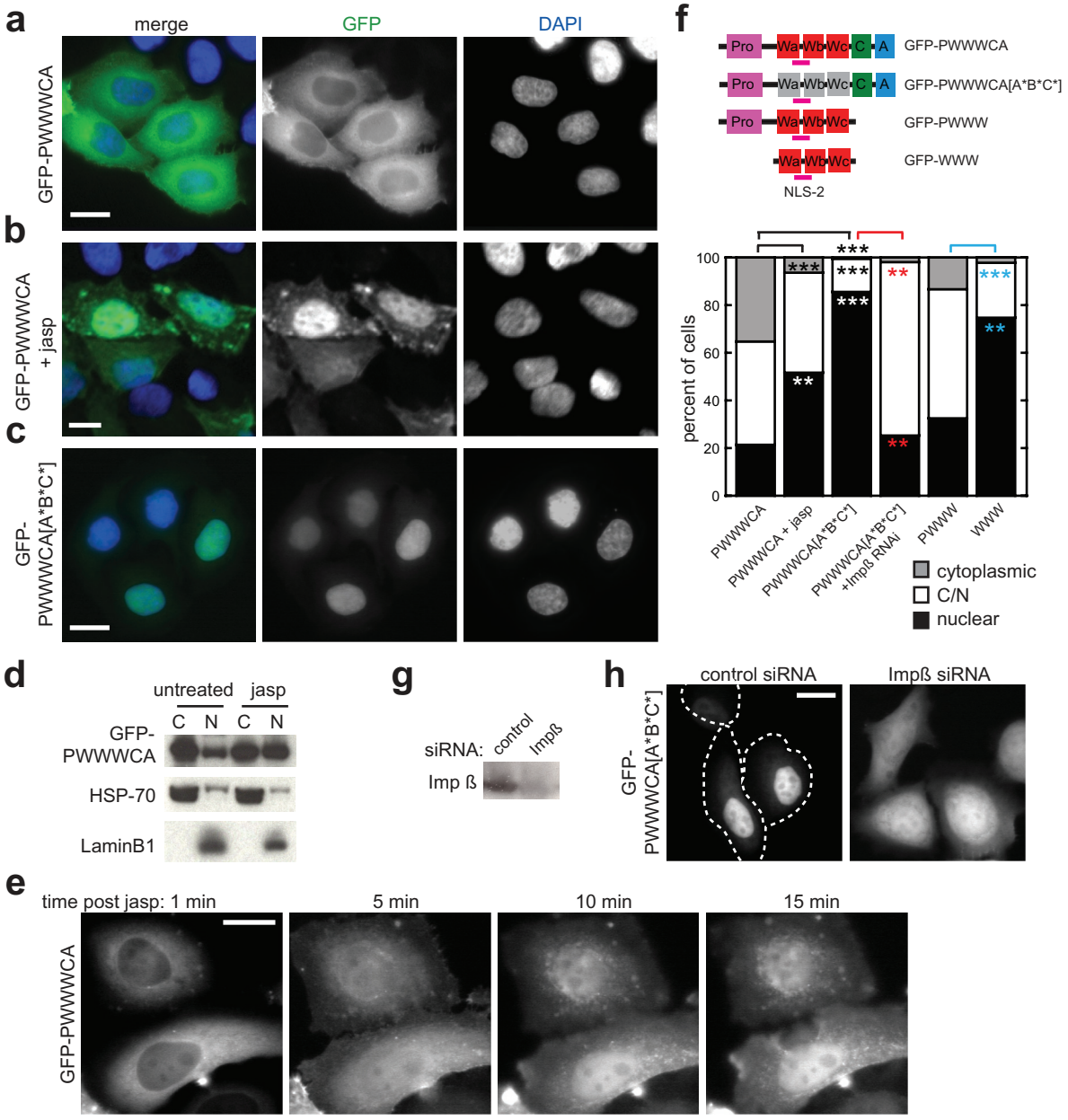

FIGURE 2: The C-terminus of JMY recapitulates actin-dependent localization. (A–C) Whereas GFP-PWWWCA is largely cytoplasmic (A), it accumulates in the nucleus following polymerization of actin with jasp (B) or when actin binding is blocked with WH2 point mutations (GFP-PWWWCA[A*B*C*]; C). Cells transiently transfected with GFP constructs were treated for 30 min with jasp as marked, then fixed and imaged. (D) Cellular fractionations as in Figure 1B show accumulation of GFP-PWWWCA in the nucleus following jasp treatment. (E) Time-lapse microscopy of GFP-PWWWCA following addition of 500 nM jasp. All scale bars, 20 μm. (F) Top, diagram showing C-terminal JMY fragments. Bottom, quantification of microscopy in (a–h); >150 cells per condition, n = 3. **p < 0.01; ***p < 0.005. Conditions are compared with GFP-PWWWCA alone, except where indicated with colored brackets. C/N, equally distributed in cytoplasm and nucleus. (G, H) Impβ is required for nuclear localization of the GFP-PWWWCA[A*B*C*] mutant. (G) Immunoblot showing that Impβ expression was knocked down by RNAi with an Impβ-specific siRNA but not control siRNA (see also Supplemental Figure S5, a). (H) RNAi of Impβ, but not control siRNA, causes GFP-PWWWCA[A*B*C*] localization to shift from exclusively nuclear to equally distributed between the nucleus and cytoplasm. This demonstrates that its normal nuclear localization is dependent on Impβ.

Actin-dependent localization of JMY is recapitulated by GFP-PWWWCA

We next asked whether the C-terminal (PWWWCA, where P stands for polyproline domain) region of JMY, which contains both the actin-binding WH2 domains and NLS-2, is sufficient for actin-dependent nuclear accumulation. Similar to full-length GFP-JMY, GFP-PWWWCA is largely cytoplasmic, or equally distributed between the nucleus and cytoplasm, in most cells (only 21.4 ± 3.0% nuclear; Figure 2, A and F). It rapidly accumulates in the nucleus in response to actin polymerization by jasp, and its accumulation is more robust than that for full-length JMY (6.5 ± 0.2% cytoplasmic, 51.8 ± 5.1% nuclear in jasp-treated cells; Figure 2, B and F). Cellular fractionation confirms this observation (Figure 2D), and time-lapse microscopy demonstrates that GFP-PWWWCA accumulates in the nucleus after

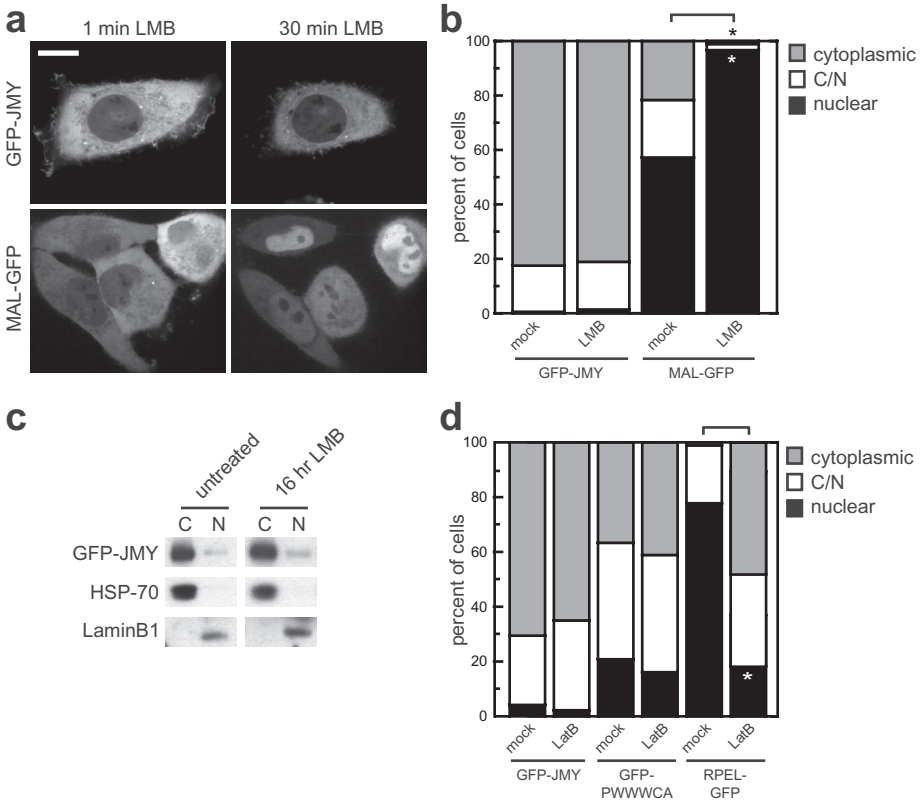

FIGURE 3: Nuclear accumulation of JMY is not regulated by export. (A–C). GFP-JMY does not accumulate in the nucleus following inhibition of Crm-1–dependent nuclear export by LMB. (A) Cells transiently transfected with GFP-JMY or MAL-GFP (control) were imaged immediately and 30 min after adding LMB. GFP-JMY remains in the cytoplasm, whereas MAL-GFP rapidly accumulates in the nucleus. Scale bars, 20 μm. (B) Transiently transfected cells were treated with LMB as marked for 30 min, fixed, and imaged. LMB does not induce nuclear accumulation of JMY. In contrast, MAL-GFP is significantly more nuclear following LMB treatment. *p <0.05. More than100 cells per condition, n = 2. (C) Cellular fractionations show that JMY does not accumulate in the nucleus of cells grown overnight in the presence of LMB. (D) LatB drives export of RPEL-GFP but not of GFP-JMY or GFP-PWWWCA. *p <0.05; >100 cells per condition, n = 3 for all conditions, except GFP-PWWWCA + Lat and RPEL-GFP + Lat, n = 2. C/N, equally distributed in cytoplasm and nucleus.

just 10–15 min of treatment (Figure 2E). WH2 point mutations that block actin binding (GFP-PWWWCA[A*B*C*]) cause JMY localization to become almost entirely nuclear (85.1% nuclear; Figure 2, C and F). Of interest, although PWWW (lacking the CA domain) behaves similarly to PWWWCA (32.4 ± 3.0% nuclear), removing the polyproline domain (WWW) decreases the fraction of cells with nuclear JMY to 74.8 ± 0.5% (Figure 2F and Supplemental Figure S3A; see *Discussion*).

Is the nuclear localization of GFP-PWWWCA[A*B*C*] dependent on the classical nuclear import machinery of Impα and Impβ? Humans have several Impα paralogues but only one Impβ (Quensel *et al.*, 2004), so to test this we knocked down Impβ expression by RNAi (Figure 2G; see also Supplemental Figure S5A). In cells treated with Impβ small interfering RNA (siRNA), but not control siRNA, GFP-PWWWCA[A*B*C*] loses its strict nuclear localization (Figure 2, F and H). This suggests that nuclear accumulation of JMY is due to regulated import and not diffusion through the nuclear pore.

Nuclear localization of JMY is not regulated by export

In addition to controlling the rate of nuclear import of JMY, does actin also control the rate of export? Our observation that actin polymerization causes JMY to accumulate in the nucleus can be explained by polymerization inducing either 1) an increase in the rate of nuclear import or 2) a decrease in the rate of nuclear export. For decreased export to promote nuclear accumulation, JMY would have to normally shuttle between the cytoplasm and nucleus. Arguing against the second model, we found that neither endogenous nor GFP-JMY accumulates in the nucleus after export is blocked with LMB for 30 min (GFP-JMY from 1.2 ± 0.7% nuclear to 1.3 ± 0.7% nuclear; Figure 3, A and B). Immunoblots of fractionated cells reveal no nuclear accumulation of GFP-JMY even when cells are grown overnight with LMB (Figure 3C). In contrast, MAL accumulates in the nucleus immediately after blocking of nuclear export with LMB (Vartiainen *et al.*, 2007; Figure 3, A and B). This suggests that JMY does not normally shuttle between the cytoplasm and nucleus. JMY has no putative nuclear export signal (la Cour *et al.*, 2004), but it remains possible that its export from the nucleus is independent of Crm-1 but dependent on actin. Depolymerizing actin with LatB induces cytoplasmic localization of MAL or the MAL RPEL cluster but has no significant effect on full-length GFP-JMY or GFP-PWWWCA (Figure 3D). This is also true in DNA-damaged cells, in which basal GFP-JMY localization is more nuclear (Supplemental Figure S3B). Thus, export of JMY is not regulated by actin monomers.

Actin and importins compete for binding to JMY

The spatial overlap between the importin-binding NLS and actin-binding WH2 domains (Supplemental Figure S2C) suggests a model for how actin regulates JMY nuclear import. Do actin monomers inhibit import of JMY by directly competing with the binding of importins? We developed a glutathione *S*-transferase (GST) pulldown assay that allows us to simultaneously detect binding of actin monomers, Impα, and Impβ to GST-tagged JMY WWWCA or GST alone. Actin and importins bind to GST-JMY, whereas very little binds nonspecifically to GST alone (Figure 4, A and B). Titrating the actin monomer concentration shows that actin effectively competes Impα/β off of GST-JMY (Figure 4, C and D). Competition is dose dependent and saturates at ~10 μM, approximately the same concentration at which actin binding saturates. Using depletion of Impα/β from the supernatant as an indirect readout of binding affinity, we confirmed that actin competes with binding of Impα/β to JMY (Supplemental Figure S3G). Competition is greatly attenuated when the affinity for actin binding to WH2-a and WH2-b is weakened using the same mutations as in Figure 1 (see Supplemental Figure S3, C and D).

Impα is normally autoinhibited but becomes able to bind an NLS following binding of Impβ (Fanara *et al.*, 2000; Catimel *et al.*, 2001). Accordingly, Impα does not bind to GST-JMY in the absence of Impβ, demonstrating that the binding we see in the presence of the Impα/β complex is specific (Figure 4, A and B). Impβ, however, binds directly to GST-JMY in the absence of Impα. Although NLSs

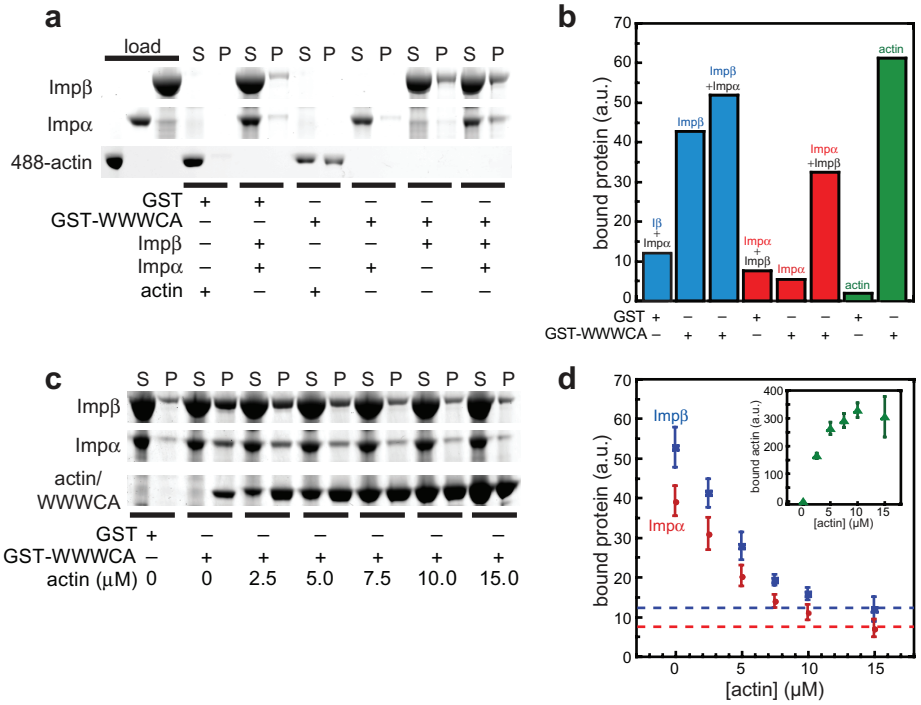

FIGURE 4: Importins and actin compete for binding to JMY. (A, B) GST pulldown showing that actin, Impα, and Impβ bind to JMY GST-WWWCA. Following incubation of purified proteins with GST-WWWCA glutathione–Sepharose beads, the supernatant (S) was removed, the beads were washed, and bound proteins (P) were eluted. Actin (5% Alexa 488 labeled) was kept monomeric by the inclusion of 2× molar excess of LatB. Impβ binds even in the absence of Impα, but Impα binds only in the presence of Impβ, consistent with it being autoinhibited (Fanara *et al.*, 2000). GST alone is used to show background, which is largely nonspecific binding to the resin. SDS–PAGE gels were first scanned for Alexa 488 actin and then stained with SYPRO Red to visualize proteins (see also full gel scan in Supplemental Figure S4, f). (B) Bound proteins were quantified using ImageQuant software. (C, D) Actin competes with Impα/β for binding to JMY. GST-WWWCA beads were incubated with 2.5 μM Impα and Impβ and increasing concentrations of LatB-actin. By 10–15 μM actin, actin binding has saturated and bound importin levels have been reduced to the level of nonspecific binding. (D) Quantification of bound Impα and Impβ, showing the averages from three independent experiments. Inset, bound actin. Error bars, SEM.

are typically bound directly by Impα, some arginine-rich NLSs (like JMY NLS-2) also interact directly with Impβ (Palmeri and Malim, 1999; Fontes *et al.*, 2003).

Because actin and importins compete for binding to JMY and Impβ is sufficient to bind JMY, does Impβ block actin nucleation by JMY? We find that Impβ markedly decreases the rate of JMY-catalyzed actin polymerization in vitro but has no effect on actin polymerization in the absence of JMY or on Arp2/3 activation by a C-terminal fragment of JMY (WCA) lacking NLS-2 (Supplemental Figure S3, E and F, and data not shown). Nucleation activity is not completely blocked, and the decrease in activity saturates at approximately the same activity as a JMY fragment lacking WH2-a (JMY WWCA), suggesting that, at least in vitro, importins are only able to block actin from binding to WH2-a.

On the basis of these results, we tested whether this competition mechanism is conserved between JMY and MAL. MAL binds actin monomers using a cluster of three RPEL motifs (Miralles *et al.*, 2003; Guettler *et al.*, 2008) that overlap with a functional NLS (Vartiainen *et al.*, 2007). Like JMY, MAL accumulates in the nucleus when actin polymerizes. We find that purified actin and importins also compete for binding to the MAL RPEL cluster (Supplemental Figure S5, A–E), consistent with recent findings (Pawłowski *et al.*, 2010). Unlike JMY, MAL does not nucleate actin (Supplemental Figure S4F). These results demonstrate that actin regulates JMY and MAL localization by the same mechanism: competing with importins for direct binding.

Importins and actin binding control DNA damage–induced nuclear accumulation of JMY

The established nuclear role of JMY is as a transcriptional coactivator of p53. DNA damage causes both increase in JMY expression and accumulation of JMY in the nucleus, where it potentiates p53-dependent transcription of proapoptotic genes (Shikama *et al.*, 1999; Coutts *et al.*, 2007). Does DNA damage trigger JMY localization to the nucleus by the same mechanism as the actin polymerization-induced accumulation that we have described? Recent work from several groups revealed that DNA damage induces polymerization of cytoplasmic actin (Levee *et al.*, 1996; Guerra *et al.*, 2008; Croft *et al.*, 2011; Ishimoto *et al.*, 2011). These studies were conducted using multiple cell types and genotoxic agents, suggesting that actin polymerization is a general response to DNA damage. On the basis of these results, we tested whether UV-induced DNA damage also promotes actin filament assembly. It is striking that we found that following DNA damage, actin polymer concentrations (measured by average cellular intensity of Alexa 568–phalloidin) nearly double (568–phalloidin intensity: untreated, 1.0 ± 0.04 arbitrary fluorescence units; 12 h post-UV, 1.4 ± 0.2; 24 h post-UV, 1.8 ± 0.1; Figure 5, A and B). Of importance, the UV treatment conditions that induce actin polymerization are identical to those that cause JMY nuclear accumulation.

JMY accumulates in the nucleus following DNA damage caused by multiple agents, including UV irradiation, etoposide, and neocarzinostatin (Figure 5, C and D, and Supplemental Figure S5; see also Supplemental Figure S3B). Following UV treatment, GFP-JMY is predominantly nuclear in 54.6 ± 3.2% of cells, compared with 4.1 ± 1.4% of control cells. As expected, DNA damage–induced nuclear import of JMY requires Impβ (following UV treatment JMY is predominantly nuclear in only 2.6 ± 1.6% of Impβ RNAi cells; Supplemental Figure S5, A–C). In contrast to full-length JMY, the truncation mutant ΔWWWCA does not accumulate in the nucleus in response to UV (percentage nuclear: pre-UV, 0.0 ± 0%; post-UV, 0.4 ± 0.4%; Figure 5, C and D) or etoposide (Supplemental Figure S5, D and E), demonstrating that this region, which contains NLS-2 (but not NLS-1), is required for DNA damage–induced nuclear import. The truncation mutant ΔCA, which lacks its Arp2/3-binding site but still contains NLS-2 and the WH2 domains, is indistinguishable from full-length JMY (Supplemental Figure S5D). Together, these results suggest that DNA damage causes JMY nuclear accumulation by driving actin polymerization, which reduces actin monomers bound to JMY and allows for importin-dependent nuclear import.

DISCUSSION

Previous work demonstrated that, in response to DNA damage, JMY accumulates in the nucleus and promotes p53-mediated

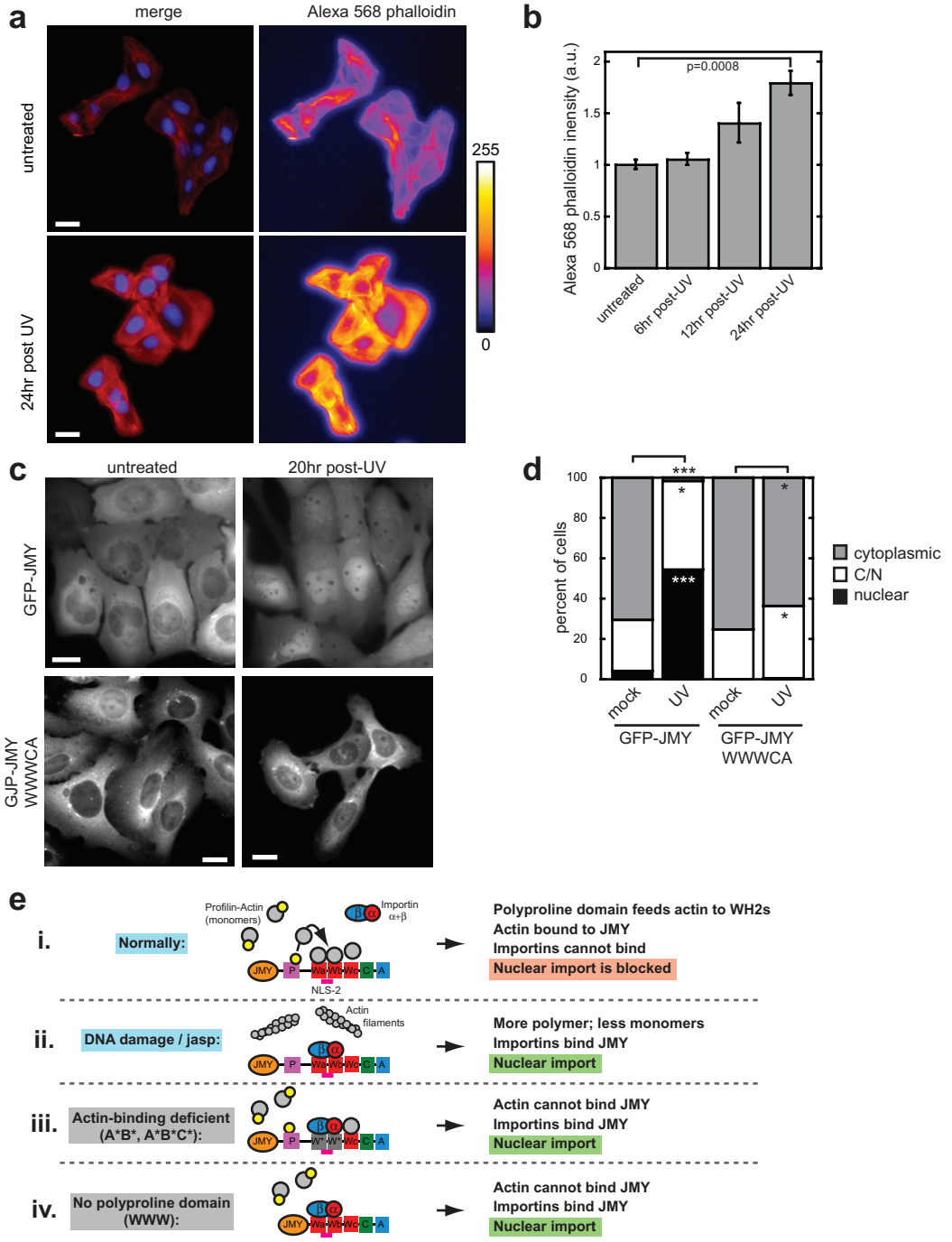

FIGURE 5: Importins and actin binding control DNA damage–induced nuclear accumulation of JMY. (A, B) Actin polymerizes in U2OS cells in response to DNA damage induced by UV irradiation (50 J/m^2). Cells were treated with UV at staggered start times and fixed at the same time and then stained with Alexa 568–phalloidin (see *Materials and Methods*). (A) Untreated cells (top) and cells 24 h after UV treatment (bottom). Left, merged images of Alexa 568–phalloidin and DAPI. Right, Alexa 568–phalloidin images are false colored to show intensity (ImageJ). Scale bars, 5 μm. (B) Quantification of average cellular Alexa 568–phalloidin intensity in cells without and at several time points after UV treatment. n = 4 coverslips, on two separate days. (C, D) GFP-JMY, but not ΔWWWCA, accumulates in the nucleus in response to DNA damage induced by UV irradiation. Cells stably expressing GFP-JMY or GFP-JMYΔWWWCA (Zuchero *et al.*, 2009) were imaged before and 20 h after UV treatment (50 J/m^2). Scale bars, 10 μm. (D) Quantification of >240 cells per condition, n = 3. C/N, equally distributed in cytoplasm and nucleus. *p <0.05, ***p <0.005. (E) Model of how actin regulates nuclear import of JMY. (i) In untreated cells, the polyproline domain feeds free actin monomers to JMY WH2 domains, which blocks binding of importins, keeping JMY in the cytoplasm. (ii) Following DNA damage or treatment with jasp, actin polymerizes. This decreases the concentration of free monomer and allows importins to bind JMY and import it into the nucleus. (iii) In the case of actin-binding mutants (e.g., GFP-JMY[A*B*]), importins can constitutively bind and import JMY into the nucleus. (iv) JMY lacking the polyproline domain may be unable to bind actin monomers, making this mutant equivalent to actin binding–deficient mutants.

apoptosis. We find that this DNA damage–induced nuclear accumulation requires a nuclear localization sequence in JMY buried within a cluster of actin monomer-binding sites. We also find that monomeric actin regulates JMY's nuclear import by blocking interaction with the import machinery. These results argue that nuclear accumulation of JMY may be triggered by DNA damage–induced actin assembly. Consistent with this idea, we observed that DNA damage induces robust actin polymerization, nearly doubling the filamentous actin concentration in the cytoplasm and significantly reducing the concentration of monomeric actin. This observation fits with previous studies demonstrating DNA damage–induced actin assembly (Levee *et al.*, 1996) and identifying a Rho-dependent pathway that links DNA damage to actin filament assembly (Croft *et al.*, 2005, 2011).

Is it possible that JMY's localization is dependent on binding to filamentous actin? We showed previously that, in vitro, JMY binds monomeric actin but does not appreciably copellet with filamentous actin or cap filament ends (Zuchero *et al.*, 2009). In cells JMY does not localize strongly to actin-rich structures such as stress fibers, nor does depolymerizing actin filaments with LatB affect JMY localization. Together these results argue that actin filaments do not directly influence JMY's subcellular localization.

The localization of both JMY and the MRTF family member MAL is determined by competition between actin monomers and the nuclear import machinery, but regulation of the two proteins is not identical. For example, when MAL is concentrated in the nucleus, treatment of cells with latrunculin B causes it to move into the cytoplasm (Vartiainen *et al.*, 2007; Figure 3D), consistent with the fact that MAL shuttles continuously between the two compartments and can be trapped in the cytoplasm by association with newly liberated actin monomers. In contrast, latrunculin does not deplete JMY from nuclei of cells with damaged DNA (Supplemental Figure S3B), consistent with our observation that JMY does not cycle between nucleus and cytoplasm (Figure 3, A–C). Why does MAL cycle between nucleus and cytoplasm, whereas JMY does not? The difference could reflect tighter inhibition of nuclear import by the WH2–actin complexes of JMY than that of the RPEL–actin complexes of MAL, or it could reflect stable association of JMY with nuclear partners, perhaps components of the DNA damage response (Shikama *et al.*, 1999; Demonacos *et al.*, 2001).

The lack of continuous cycling means that once JMY is in the nucleus its localization is insensitive to changes in cytoplasm actin. In this way JMY's nuclear localization performs like a toggle switch: a transient dip in monomeric actin concentration produces prolonged nuclear accumulation. This is probably important for its cellular function. For example, JMY promotes initiation of apoptosis and, early in this process, the concentration gradient of Ran-GTP between the nucleoplasm and cytoplasm collapses, trapping many NLS-containing proteins in the cytoplasm bound to Impα/β (Wong *et al.*, 2009). If JMY shuttled back and forth, it would not remain in the nucleus of apoptotic cells. In later stages of apoptosis the concentration of monomeric actin increases (Suarez-Huerta *et al.*, 2000), which would also trap rapidly shuttling JMY molecules in the cytoplasm.

Once in the nucleus, does actin also contribute to JMY-mediated transcription? Coutts *et al.* (2009) found that JMY targeted to the nucleus with an NLS stimulates p53-dependent transcription of a reporter gene, and LatB blocks this. This suggests that the role of JMY in transcription either requires actin polymerization or is inhibited by actin monomers. Now that actin- and Arp2/3–binding mutants of JMY have been characterized, it will be interesting to test whether JMY promotes actin polymerization in the nucleus and whether it requires this for its role in activating p53. We show here that different actin-binding mutations can perturb the localization of JMY, so it will be essential to take this into consideration when comparing the phenotypes of mutants.

How is JMY's actin assembly activity regulated in cells? Recent cell biological experiments suggest that, in vivo, JMY activity is regulated by interaction with inhibitory binding partners. One obvious potential regulator is the nuclear import machinery, specifically the importin α/β complex (Supplemental Figure S4, D and E). The inhibitory effect of Impβ, however, relies on direct competition with monomeric actin, which has a cytoplasmic concentration at least 20-fold higher than that of Impβ (Gordon *et al.*, 1976; Görlich *et al.*, 1994). It is therefore extremely unlikely that importins regulate JMY activity in vivo.

Of interest, JMY requires its polyproline domain for retention in the cytoplasm (Figure 2F and Supplemental Figure S3A). Most proteins that activate the Arp2/3 complex contain a polyproline domain N-terminal to the WCA region (Rottner *et al.*, 2010), and it is believed that polyproline domains facilitate the recruitment of profilin-bound actin monomers to Arp2/3 activators (Witke, 2004). Because the polymerizable pool of actin monomers in cells is largely bound to profilin (Kaiser *et al.*, 1999), without the polyproline sequence it is possible that occupancy of the WH2 domains by actin is low, making this mutant equivalent to PWWWCA[A*B*C*]. Thus JMY could potentially be regulated by a protein that binds directly to its polyproline domain.

In addition to JMY and MAL, we identified 26 other actin-binding proteins with putative NLSs. It will be interesting to test whether any of these plays a role in actin assembly in the nucleus. Of particular interest are the 14 with overlap between ABD and NLS. Although most do not appear to shuttle in an actin-dependent manner, it is possible that their actin-regulatory activities are regulated by importin binding (and RanGTP). This could allow for control of their activities in the interphase nucleus or around mitotic chromosomes, similar to spindle factors, including the microtubule-organizing proteins TPX2 (Gruss *et al.*, 2001) and NuMA (Nachury *et al.*, 2001; Wiese *et al.*, 2001), and nuclear lamins (Tsai *et al.*, 2006). Future work will test the role of these proteins in coupling actin dynamics with nuclear and mitotic events.

MATERIALS AND METHODS

Bioinformatics

Canonical domain alignments of well-characterized ABDs, including monomer-binding families (WH2, RPEL) and filament-binding families (calponin homology, formin homology 2, ILWEQ, ezrin/radixin/moesin), were generated from published alignments supplemented with results of a high-stringency National Center for Biotechnology Information (NCBI) protein Basic Local Alignment Search Tool (pBLAST) search (e value, <0.00001) to ensure alignment diversity. Human proteins containing putative ABDs were identified using a low-stringency NCBI BLASTp search (e value, <0.05) based on similarity to members of canonical domain alignments. ABD- and NLS-containing candidates were identified from these results based on the presence of 1) one or more sequence motifs identified by NLS regular expression patterns from the NLSdb (http://rostlab.org/services/nlsdb/), 2) detectable conservation within the characterized actin-binding sites within each ABD using BLASTp (e value, <0.00001 for actin-binding sites >50 residues in length; any detectable similarity for actin-binding sites <50 residues), and 3) <5 residues of separation between putative NLS and ABD regions.

Molecular biology

Constructs were cloned from full-length mouse JMY or MAL using standard techniques. Primer sequences are available upon request.

JMY mutations are as follows: A*B*C* refers to triplicate mutations in each WH2 to block actin binding, in WH2-a (LF857AA, L870A), WH2-b (VL889AA, L900A), and WH2-c (IL920AA, L930A). Amino acid numbers of JMY constructs are as follows: GFP-PWWWCA, 791–983; GFP-PWWW, 791–938; GFP-WWW, 853–938; GFP-JMYΔCA, 1–938; GFP-JMYΔWWWCA, 1–852. MAL constructs are as follows: full-length MAL-GFP, 1–1021; RPEL-GFP, 2–261. The numbering of mouse MAL begins at leucine –92 (Miralles *et al.*, 2003). All constructs were sequenced to ensure no mutations were introduced during cloning. We used pEGFP-C1 and pEGFP-N3 (Clontech, Mountain View, CA) as host vectors for making enhanced GFP fusions.

Cell culture

HeLa and U2OS cells (American Type Culture Collection, Manassas, VA) were cultured in DMEM supplemented with 10% fetal bovine serum, 2 mM L-glutamine, nonessential amino acids, and penicillin–streptomycin (University of California, San Francisco, Cell Culture Facility, San Francisco, CA) at 37°C with 5% CO_2. For transfection, cells were seeded onto glass coverslips overnight and transfected with GFP constructs using Lipofectamine LTX (Invitrogen, Carlsbad, CA), according to the manufacturer's protocol. For Impβ1 RNAi, GFP-JMY stable cells (Zuchero *et al.*, 2009) were transfected with 100 nM nontargeting (Stealth Medium GC#2; Invitrogen) or Impβ1 siRNA (targeting bases 497–521 of human Impβ mRNA; Miki *et al.*, 2008; purchased from Invitrogen), using Lipofectamine 2000 according to manufacturer's protocols, and grown for 3 d prior to UV treatment. Alternatively, siRNA and plasmid DNA were cotransfected using Lipofectamine 2000. For immunofluorescence, cells were fixed for 30 min in 3.2% formaldehyde in phosphate-buffered saline (PBS). Cells were then permeabilized with 0.1% Triton-X-100 in PBS, and nuclei were stained with 0.5 µg/ml 4′,6-diamidino-2-phenylindole (DAPI; Sigma-Aldrich, St. Louis, MO). Fixed samples were mounted with fluorescent mounting medium (DakoCytomation, Hamburg, Germany).

Microscopy

Epifluorescence and wide-field images were acquired on a TE300 inverted microscope (Nikon, Melville, NY) equipped with a Hamamatsu C4742-98 cooled charge-coupled device camera (Hamamatsu, Hamamatsu, Japan), using 100× and 60×, 1.4 numerical aperture, Plan Apo objectives (Nikon) with MicroManager software (Stuurman *et al.*, 2007). We used ImageJ (National Institutes of Health, Bethesda, MD) and Adobe Photoshop (Adobe, San Jose, CA) for image analysis and contrast adjustment. For live-cell imaging, cells were transfected, split onto glass coverslips after 18–24 h, and then given fresh medium with drugs or vehicle and kept at 37°C during image acquisition. Stable lines of U2OS cells expressing GFP-JMY were described previously (Zuchero *et al.*, 2009). Localization of GFP fusion proteins was scored as predominantly cytoplasmic, equally distributed between the cytoplasm and nucleus (C/N), or predominantly cytoplasmic by an observer blind to the experimental condition (Guettler *et al.*, 2008). Percentages presented in the text refer to percentage of cells in each category, unless otherwise indicated.

Drug treatments and UV irradiation

Jasplakinolide (Calbiochem, La Jolla, CA) and latrunculin B (Biomol International, Enzo Life Sciences, Plymouth, PA) were used at 500 nM in medium, and treatments were for 30 min. Leptomycin B (Sigma-Aldrich) was used at 20 nM for 30 min or 16 h, as noted. Etoposide (Sigma-Aldrich) was used at 10 µM, and neocarzinostatin (Sigma-Aldrich) was used at 200 ng/ml. We made working stocks of all drugs or vehicle (dimethyl sulfoxide for LatB and jasp; methanol for LMB) in warm medium, replaced old medium with drugged medium, and incubated for the given time at 37° with 5% CO_2. Following treatment, cells were washed twice with warm PBS prior to fractionation or fixation for microscopy. For UV irradiation, medium was fully aspirated from cells, and they were subjected to a dose of 50 J/m^2 short-wave UV (0.5 mW/cm^2 for 10 s) in a GS Genelinker UV chamber (Bio-Rad, Hercules, CA; to achieve this low fluence rate, we needed to remove bulbs from the UV chamber). Fresh, warm medium was immediately added, and cells were returned to the incubator for the indicated time before fixing for imaging.

For calculation of phalloidin intensities, U2OS cells were UV treated at staggered times, so that all conditions were fixed at the same time postplating. Cells were fixed and permeabilized as described, stained for 15 min with 0.7 U/ml Alexa Fluor 568–phalloidin (Invitrogen), washed three times, and mounted as described. Four coverslips per condition, on two separate experimental days, were imaged. Ten micrographs per coverslip (>500 cells per coverslip, spanning the entire coverslip) were acquired blindly by focusing on the DAPI channel. Average cellular phalloidin intensity was measured in regions of interest containing all cells, using ImageJ. Slide background intensity was subtracted, and values were normalized by dividing by the average intensity of untreated cells.

Cellular fractionations

Approximately 1×10^6 cells were harvested, washed with ice-cold PBS, and resuspended in hypotonic buffer (10 mM 4-(2-hydroxyethyl)-1-piperazineethanesulfonic acid [HEPES], pH 7.5, 10 mM KCl, 1.5 mM $MgCl_2$, 0.5 dithiothreitol, 5 µg/ml aprotinin, 15 µg/ml benzamidine, 10 µg/ml leupeptin, 5 µg/ml pepstatin A, 1 mM phenylmethanesulfonylfluoride, and 40 µg/ml soybean trypsin inhibitor). Cells were pelleted in a microfuge by spinning at 1000 rpm for 5 min at 4°C and then lysed on ice for 10 min in hypotonic buffer plus 0.5% NP-40. Nuclei were pelleted by spinning at 3000 rpm for 2 min as described, and cytoplasmic fraction was aspirated and held on ice. Nuclei were washed with hypotonic buffer, assessed for quality by phase contrast microscopy, transferred to a new tube, and lysed in 8 M urea plus sample buffer, then boiled and sonicated prior to SDS–PAGE. For each fractionation experiment we blotted against HSP70 (cytoplasmic marker) and lamin B1 (nuclear marker) to monitor separation of cytoplasmic and nuclear fractions. Standard methods were used for immunoblotting, using 1:500 dilutions of 1289 (Coutts *et al.*, 2007) and YA16 (Santa Cruz Biotechnology, Santa Cruz, CA) anti-JMY primary antibodies, mouse anti–lamin B1 (Invitrogen), mouse anti-HSP70 (Santa Cruz Biotechnology), 1:200 goat anti-Impβ (Santa Cruz Biotechnology), or 1:1000 mouse anti–actin JLA20 (Calbiochem). Horseradish peroxidase–conjugated secondaries (Jackson ImmunoResearch Laboratories, West Grove, PA) were used at 1:10,000, and ECL reagent (SuperSignal West Pico, Pierce, Rockford, IL) was used according to the manufacturer's instructions.

For quantification, subsaturated immunoblots were scanned (bands were deemed subsaturated if they were still translucent, i.e., text could be read through the band), and band intensity was measured and background subtracted in ImageJ. We measured relative nuclear JMY signal between jasp-treated and untreated cell lysates in the same blot. Measuring this ratio in several exposures of the same immunoblot confirmed that this ratio did not vary appreciably with different blot exposure intensities, provided they were subsaturated. Thus we could compare several experimental replicates without having to precisely match exposure intensity.

Biochemistry

JMY and MAL fragments were expressed as GST fusions in *Escherichia coli* and purified using a combination of glutathione and cation chromatography. For actin polymerization experiments the GST was removed to prevent dimerization of the recombinant protein. We used JMY(C978S) for biochemistry to improve reproducibility (Zuchero *et al.*, 2009). Recombinant NusA-hexahistidine–tagged Impβ was purified by cobalt chromatography, removal of the NusA tag by cleavage with trypsin, and gel filtration on a Superdex 200 column. Protein concentrations were calculated using predicted molar extinction coefficients for JMY peptides (ProtParam, http://web.expasy.org/protparam/) or by quantitative SDS–PAGE with SYPRO Red staining (Invitrogen).

For GST pulldowns, 10 μM GST-tagged proteins or GST alone was bound to glutathione–Sepharose 4B (GE Healthcare, Piscataway, NJ) or glutathione magnetic beads (Pierce) in PBS, 0.5 μM TCEP, and 20% glycerol, with rotation, for 2–16 h at 4°, then washed three times to remove unbound protein. Note that background binding of proteins to glutathione magnetic beads (GST-MAL experiments) is much reduced compared with glutathione–Sepharose beads (GST-JMY experiments). Loaded beads (GST fusion proteins at ~1 μM in final reaction volume) were rotated with proteins or protein storage buffer in PBS, 0.5 μM tris(2-carboxyethyl)phosphine (TCEP), and 5 mg/mL bovine serum albumin (carrier) for 2–3 h at 4°C. As noted, 2.5 μM each Impα and Impβ was used. Actin was kept monomeric by using 2× molar equivalent of LatB. Beads were pelleted by centrifugation or magnetic separation, supernatant removed, and washed three times with PBS + 0.01% NP-40, transferring to a new tube in the final wash to prevent eluting protein nonspecifically adsorbed to the tube wall. Bound proteins were recovered in sample buffer (same volume as reactions), and samples were analyzed by SDS–PAGE (NuPage gradient gels; GE Healthcare) with SYPRO Red staining and quantified by using a multiformat imager (Typhoon 9400; GE Healthcare) and ImageQuant software (GE Healthcare). SYPRO Red binds to SDS, and thus the measured fluorescence reflects mass of protein; we divided values by the molecular weight of the protein (42,000 Da for actin, 97,000 Da for Impβ, and 60,000 Da for Impα) to calculate bound protein in relative molar terms. For visualization of Alexa 488–labeled actin, gels were scanned (Typhoon 9400) prior to SYPRO Red staining.

Actin polymerization assays

Actin was purified from *Acanthamoeba castellanii* as described (Gordon *et al.*, 1976), labeled with pyrene iodoacetamide or Alexa 488 C5 maleimide as described (Cooper *et al.*, 1983; Akin and Mullins, 2008), stored in buffer A (0.2 mM ATP, 0.5 mM TCEP, 0.1 mM $CaCl_2$, 0.02% wt/vol sodium azide, 2 mM Tris, pH 8.0, at 4°C), and gel filtered before use. *Acanthamoeba* actin is 95.5% identical, 99.2% conserved with regard to human β-actin (compared with human or rabbit skeletal muscle actin, 92.8% identical), and so represents a better model of cytoplasmic actin than skeletal muscle actin. Arp2/3 was purified from *Acanthamoeba* as described (Dayel *et al.*, 2001) and flash frozen with 10% glycerol. Actin polymerization assays were performed as described (Zuchero *et al.*, 2009) in 1× KMEH (50 mM KCl, 1 mM $MgCl_2$, 1 mM ethylene glycol tetraacetic acid [EGTA], 10 mM HEPES, pH 7.0). Ca^{2+}-actin was converted into Mg^{2+}-actin by incubation of actin in ME (50 mM $MgCl_2$, 0.2 mM EGTA) for 2 min prior to adding 10× KMEH and test components. Pyrene fluorescence was measured with a Synergy 4 plate reader and Gen5 software (BioTek, Winooski, VT). Unless otherwise noted, polymerization reactions contained 4 μM actin (5% pyrene labeled) and 250 nM JMY. Importin competition reactions contained 200 nM CT-JMY (amino acids 583–983, encompassing both NLS sequences) and 5 μM Impβ or an equivalent volume of Impβ storage buffer. For half-time calculations, reactions were normalized by zeroing traces, dividing by the plateau value, and solving for time at half-maximal fluorescence (0.5 a.u.). All error values are SEM. We used two-tailed unpaired *t* tests, assuming unequal variance, to calculate p values (Excel; Microsoft, Redmond, WA).

ACKNOWLEDGMENTS

This work began in the 2008 Physiology Course at the Marine Biological Laboratory in Woods Hole with the talents and creativity of D. Shane Courson, P. Myron Miller, and H. Hewitt Tuson. We are greatly indebted to Yoshihiro Yoneda, Takashi Miki, and Peter Bieling for advice and generously providing importin constructs and proteins. This work was supported by grants from the National Institutes of Health, an American Heart Association Predoctoral Fellowship (J.B.Z.), the Robert Day Allen Fellowship Fund (J.B.Z.), and a National Science Foundation Predoctoral Fellowship (B.B.). We thank members of the Mullins and Vale labs, especially Orkun Akin, Scott Hansen, and Ron Vale, as well as Margot Quinlan and the Cell Division Group at the Marine Biological Laboratory, for reagents, helpful discussions, and critical reading of the manuscript.

REFERENCES

Akin O, Mullins RD (2008). Capping protein increases the rate of actin-based motility by promoting filament nucleation by the Arp2/3 complex. Cell 133, 841–851.

Bubb MR, Senderowicz AM, Sausville EA, Duncan KL, Korn ED (1994). Jasplakinolide, a cytotoxic natural product, induces actin polymerization and competitively inhibits the binding of phalloidin to F-actin. J Biol Chem 269, 14869–14871.

Bubb MR, Spector I, Beyer BB, Fosen KM (2000). Effects of jasplakinolide on the kinetics of actin polymerization. An explanation for certain in vivo observations. J Biol Chem 275, 5163–5170.

Catimel B, Teh T, Fontes MR, Jennings IG, Jans DA, Howlett GJ, Nice EC, Kobe B (2001). Biophysical characterization of interactions involving importin-alpha during nuclear import. J Biol Chem 276, 34189–34198.

Cooper JA, Walker SB, Pollard TD (1983). Pyrene actin: documentation of the validity of a sensitive assay for actin polymerization. J Muscle Res Cell Motil 4, 253–262.

Coutts AS, Boulahbel H, Graham A, La Thangue NB (2007). Mdm2 targets the p53 transcription cofactor JMY for degradation. EMBO Rep 8, 84–90.

Coutts A, Weston L, La Thangue NB (2009). A transcription co-factor integrates cell adhesion and motility with the p53 response. Proc Natl Acad Sci USA 106, 19872–19877.

Croft DR, Coleman ML, Li S, Robertson D, Sullivan T, Stewart CL, Olson MF (2005). Actin-myosin-based contraction is responsible for apoptotic nuclear disintegration. J Cell Biol 168, 245–255.

Croft DR *et al.* (2011). p53-mediated transcriptional regulation and activation of the actin cytoskeleton regulatory RhoC to LIMK2 signaling pathway promotes cell survival. Cell Res 21, 666–682.

Dayel MJ, Holleran EA, Mullins RD (2001). Arp2/3 complex requires hydrolyzable ATP for nucleation of new actin filaments. Proc Natl Acad Sci USA 98, 14871–14876.

Demonacos C, Krstic-Demonacos M, La Thangue NB (2001). A TPR motif cofactor contributes to p300 activity in the p53 response. Mol Cell 8, 71–84.

Fanara P, Hodel MR, Corbett AH, Hodel AE (2000). Quantitative analysis of nuclear localization signal (NLS)-importin alpha interaction through fluorescence depolarization. Evidence for auto-inhibitory regulation of NLS binding. J Biol Chem 275, 21218–21223.

Firat-Karalar EN, Hsiue PP, Welch MD (2011). The actin nucleation factor JMY is a negative regulator of neuritogenesis. Mol Biol Cell 22, 4563–4574.

Fontes MR,, Teh T, Jans D, Brinkworth RI, Kobe B (2003). Structural basis for the specificity of bipartite nuclear localization sequence binding by importin-alpha. J Biol Chem 278, 27981–27987.

Gordon DJ, Eisenberg E, Korn ED (1976). Characterization of cytoplasmic actin isolated from *Acanthamoeba castellanii* by a new method. J Biol Chem 251, 4778–4786.
Görlich D, Prehn S, Laskey LA, Hartmann E (1994). Isolation of a protein that is essential for the first step of nuclear protein import. Cell 79, 767–778.
Gruss OJ, Carazo-Salas RE, Schatz CA, Guarguaglini G, Kast J, Wilm M, Le Bot N, Vernos I, Karsenti E, Mattaj IW (2001). Ran induces spindle assembly by reversing the inhibitory effect of importin alpha on TPX2 activity. Cell 104, 83–93.
Guerra L, Carr HS, Richter-Dahlfors A, Masucci MG, Thelestam M, Frost JA, Frisan T (2008). A bacterial cytotoxin identifies the RhoA exchange factor Net1 as a key effector in the response to DNA damage. PLoS One 3, e2254.
Guettler S, Vartiainen MK, Miralles F, Larijani B, Treisman R (2008). RPEL motifs link the serum response factor cofactor MAL but not myocardin to Rho signaling via actin binding. Mol Cell Biol 28, 732–742.
Ishimoto T, Ozawa T, Mori H (2011). Real-time monitoring of actin polymerization in living cells using split luciferase. Bioconjug Chem 22, 1136–1144.
Kaiser DA, Vinson VK, Murphy DB, Pollard TD (1999). Profilin is predominantly associated with monomeric actin in *Acanthamoeba*. J Cell Sci 112, 3779–3790.
Kelly A, Kranitz H, Dötsch V, Mullins R (2006). Actin binding to the central domain of WASP/Scar proteins plays a critical role in the activation of the Arp2/3 complex. J Biol Chem 281, 10589–10597.
Kiuchi T, Nagai T, Ohashi K, Mizuno K (2011). Measurements of spatiotemporal changes in G-actin concentration reveal its effect on stimulus-induced actin assembly and lamellipodium extension. J Cell Biol 193, 365–380.
la Cour T, Kiemer L, Mølgaard A, Gupta R, Skriver K, Brunak S (2004). Analysis and prediction of leucine-rich nuclear export signals. Protein Eng Des Sel 17, 527–536.
Levee MG, Dabrowska MI, Lelli JL Jr, Hinshaw DB (1996). Actin polymerization and depolymerization during apoptosis in HL-60 cells. Am J Physiol 271, C1981–C1992.
Lyubimova A, Bershadsky AD, Ben-Ze'ev A (1997). Autoregulation of actin synthesis responds to monomeric actin levels. J Cell Biochem 65, 469–478.
Miki T, Okawa K, Sekimoto T, Yoneda Y, Watanabe S, Ishizaki T, Narumiya S (2008). mDia2 shuttles between the nucleus and the cytoplasm through the importin-alpha/beta- and CRM1-mediated nuclear transport mechanism. J Biol Chem 284, 5753–5762.
Miralles F, Posern G, Zaromytidou AI, Treisman R (2003). Actin dynamics control SRF activity by regulation of its coactivator MAL. Cell 113, 329–342.
Mohr D, Frey S, Fischer T, Güttler T, Görlich D (2009). Characterisation of the passive permeability barrier of nuclear pore complexes. EMBO J 28, 2541–2553.
Nachury MV, Maresca TJ, Salmon WC, Waterman-Storer CM, Heald R, Weis K (2001). Importin beta is a mitotic target of the small GTPase Ran in spindle assembly. Cell 104, 95–106.
Nair R, Carter P, Rost B (2003). NLSdb: database of nuclear localization signals. Nucleic Acids Res 31, 397–399.
Palmeri D, Malim MH (1999). Importin beta can mediate the nuclear import of an arginine-rich nuclear localization signal in the absence of importin alpha. Mol Cell Biol 19, 1218–1225.
Pawłowski R, Rajakylä EK, Vartiainen MK, Treisman R (2010). An actin-regulated importin alpha/beta-dependent extended bipartite NLS directs nuclear import of MRTF-A. EMBO J 29, 3448–3458.
Quensel C, Friedrich B, Sommer T, Hartmann E, Kohlerl M (2004). In vivo analysis of importin alpha proteins reveals cellular proliferation inhibition and substrate specificity. Mol Cell Biol 24, 10246–10255.
Quinlan ME, Heuser JE, Kerkhoff E, Mullins RD (2005). *Drosophila* Spire is an actin nucleation factor. Nature 433, 382–388.
Rottner K, Hänisch J, Campellone KG (2010). WASH, WHAMM and JMY: regulation of Arp2/3 complex and beyond. Trends Cell Biol 20, 650–661.
Sagara J, Arata T, Taniguchi S (2009). Scapinin, the protein phosphatase 1 binding protein, enhances cell spreading and motility by interacting with the actin cytoskeleton. PLoS One 4, e4247.
Shikama N, Lee CW, France S, Delavaine L, Lyon J, Krstic-Demonacos M, La Thangue NB (1999). A novel cofactor for p300 that regulates the p53 response. Mol Cell 4, 365–376.
Spector I, Shochet NR, Kashman Y, Groweiss A (1983). Latrunculins: novel marine toxins that disrupt microfilament organization in cultured cells. Science 219, 493–495.
Strasser GA, Rahim NA, VanderWaal KE, Gertler FB, Lanier LM (2004). Arp2/3 is a negative regulator of growth cone translocation. Neuron 43, 81–94.
Stuurman N, Amodaj N, Vale RD (2007). Micro-Manager: open source software for light microscope imaging. Microsc Today 15, 42–43.
Suarez-Huerta N, Mosselmans R, Dumont JE, Robaye B (2000). Actin depolymerization and polymerization are required during apoptosis in endothelial cells. J Cell Physiol 184, 239–245.
Tsai M-Y, Wang S, Heidinger JM, Shumaker DK, Adam SA, Goldman RD, Zheng Y (2006). A mitotic lamin B matrix induced by RanGTP required for spindle assembly. Science 311, 1887–1893.
Vartiainen MK, Guettler S, Larijani B, Treisman R (2007). Nuclear actin regulates dynamic subcellular localization and activity of the SRF cofactor MAL. Science 316, 1749–1752.
Welch MD, Mullins RD (2002). Cellular control of actin nucleation. Annu Rev Cell Dev Biol 18, 247–288.
Wiese C, Wilde A, Moore MS, Adam SA, Merdes A, Zheng Y (2001). Role of importin-beta in coupling Ran to downstream targets in microtubule assembly. Science 291, 653–656.
Witke W (2004). The role of profilin complexes in cell motility and other cellular processes. Trends Cell Biol 14, 461–469.
Wolff B, Sanglier JJ, Wang Y (1997). Leptomycin B is an inhibitor of nuclear export: inhibition of nucleo-cytoplasmic translocation of the human immunodeficiency virus type 1 (HIV-1) Rev protein and Rev-dependent mRNA. Chem Biol 4, 139–147.
Wong CH, Chan H, Ho CY, Lai SK, Chan KS, Koh CG, Li HY (2009). Apoptotic histone modification inhibits nuclear transport by regulating RCC1. Nat Cell Biol 11, 36–45.
Zuchero JB, Coutts AS, Quinlan ME, La Thangue NB, Mullins RD (2009). p53-cofactor JMY is a multifunctional actin nucleation factor. Nat Cell Biol 11, 451–459.